frontiers in Marine Science

ORIGINAL RESEARCH
published: 20 October 2021
doi: 10.3389/fmars.2021.680729

Vertical Nitrate Flux Induced by Kelvin–Helmholtz Billows Over a Seamount in the Kuroshio

Cristy S. Acabado[1,2,3], Yu-Hsin Cheng[4,5], Ming-Huei Chang[4] and Chung-Chi Chen[2,6]**

[1] Biodiversity Program, Taiwan International Graduate Program, Academia Sinica, Taipei, Taiwan, [2] Department of Life Science, National Taiwan Normal University, Taipei, Taiwan, [3] Institute of Marine Fisheries and Oceanology, College of Fisheries and Ocean Sciences, University of the Philippines Visayas, Iloilo, Philippines, [4] Institute of Oceanography, National Taiwan University, Taipei, Taiwan, [5] Department of Marine Environmental Information, National Taiwan Ocean University, Keelung, Taiwan, [6] College of Marine Sciences, National Dong Hwa University, Hualien, Taiwan

OPEN ACCESS

Edited by:
Hongbin Liu, Hong Kong University of Science and Technology, Hong Kong SAR, China

Reviewed by:
Takeyoshi Nagai, Tokyo University of Marine Science and Technology, Japan
Hiroaki Saito, The University of Tokyo, Japan
Gloria Silvana Durán Gómez, Tokyo University of Marine Science and Technology, Japan, in collaboration with reviewer TN

***Correspondence:**
Cristy S. Acabado
csacabado@up.edu.ph
Chung-Chi Chen
ccchen@ntnu.edu.tw

Specialty section:
This article was submitted to Marine Biogeochemistry, a section of the journal Frontiers in Marine Science

Received: *15 March 2021*
Accepted: *01 October 2021*
Published: *20 October 2021*

Citation:
Acabado CS, Cheng Y-H, Chang M-H and Chen C-C (2021) Vertical Nitrate Flux Induced by Kelvin–Helmholtz Billows Over a Seamount in the Kuroshio. Front. Mar. Sci. 8:680729. doi: 10.3389/fmars.2021.680729

Kelvin–Helmholtz (KH) billows can facilitate microscale turbulent mixing around seamounts in the Kuroshio. This study sought to describe the influence of billow intensity (i.e., "intermittent and small" and "steady and large" billows) on vertical nitrate fluxes. KH billows led to turbulent kinetic energy dissipation rates [ε = O (10^{-7} to 10^{-6}) W kg^{-1}] and eddy diffusivities [K_ρ = O (10^{-4} to 10^{-3}) m^2 s^{-1}] that were significantly stronger than those outside the billow depths. The mean nitrate flux estimated using K_ρ in the billow depths had a maximal value of 10.0 mmol m^{-2} day^{-1}, which was much higher than estimates for the open ocean. The nitrate flux associated with the shallow KH billows at two vertical levels contributed to enrich the subsurface phytoplankton maximum, while the deeper billows closer to the summit were found to induce a large amount of nitrate flux from the deeper to the subsurface water. This study showed that KH billows make important contributions to seamount ecosystems, particularly in the cycling and vertical mixing of nutrients to make them available for potential downstream transport.

Keywords: Kelvin–Helmholtz billows, nutrient, nitrate flux, seamount, the Kuroshio, turbulence

INTRODUCTION

The Kuroshio originates at the bifurcation of the North Equatorial Current, which carries oligotrophic waters low in nutrient concentrations and plankton biomass (Barkley, 1970; Kobari et al., 2020). However, several mechanisms that enhance nutrient supply and primary production in the Kuroshio have also been identified, such as its interaction with the West Philippine Sea, resulting in an evolution of Kuroshio's chemical properties (Liang et al., 2008; Chen et al., 2017, 2021). Recently, submesoscale eddies generated from the interaction of the Kuroshio with the southern tip of Taiwan have been observed to entrain high concentrations of chlorophyll *a* (Chl *a*) (Cheng et al., 2020). The Kuroshio is also affected by small islands (e.g., Green Island), that produce island wakes and enhance chlorophyll concentration (Chang et al., 2013). These reports identified a general leeward advection of chlorophyll in the Kuroshio. However, because of the complexity of the various interacting mechanisms in the upstream Kuroshio, it is difficult to determine whether nutrient enrichment downstream, particularly over seamounts, is caused exclusively by horizontal advection.

Seamounts are commonly recognized as biological hotspots in oligotrophic oceans (Uchida et al., 1986; Boehlert and Genin, 1987; Mendonca et al., 2012); however, the mechanisms behind their

productivity are still not fully understood. Ideas proposed to explain such productivity include aggregating mechanisms that concentrate Chl *a* on the seamount that were formed elsewhere, and local enhancement supported by upwelling and small-scale phenomenon that can inflate phytoplankton abundance (Genin and Boehlert, 1985; Boehlert and Genin, 1987). In the latter case, the rate of nutrient injection into the euphotic zone needs to be sufficient to impact primary productivity. Retention times depend on local hydrodynamics which are determined by seamount topography as well as the background flow conditions, so large variation among seamounts is expected (White et al., 2007). Thus, there is a need for well-founded hydrobiological information before any sound conclusion can be reached.

Since nutrient concentrations increase with depth, vertical mixing driven by small-scale physical disturbances due to flow-topography interactions over seamounts can transport dissolved inorganic nutrients into oligotrophic surface waters, creating high productivity hotspots (Biggs and Thomsen, 1995; Tsutsumi et al., 2017). To examine this phenomenon, the shallow seamounts that protrude into the core of the Kuroshio, where the flow speeds range between 1.0 and 1.5 m s^{-1}, that create a complexity of small-scale hydrodynamic disturbances, were studied (**Figure 1A**). This effort builds on the observations by Chang et al. (2016), which observed strong turbulent mixing linked to Kelvin–Helmholtz (KH) instabilities at a seamount along the Kuroshio, southeast of Taiwan.

Because KH instability explains much of the observed mixing in environmental fluids, it has been extensively studied and modeled in the atmospheric (Sckopke et al., 1981; Blumen et al., 2001) and oceanic fields (Hebert et al., 1992; Moum et al., 2003). KH instabilities are the best-known type of shear instabilities, which is a key mechanism by which the kinetic energy of the mean flow is extracted and redirected, eventually generating turbulence (Hebert et al., 1992; Smyth et al., 2001). As KH instabilities develop, they roll the denser water up from below and create a sequence of vertically circulating billows, and eventually degrade to turbulent masses as billows collapse. The collapse of the billows stimulates intensive mixing, particularly between the background fluid and that in the periphery of the billow cores (Patterson et al., 2006). As a result, the water properties such as the temperature, salinity, and chemical/biological parameters can be widely dispersed *via* the turbulent mixing. However, biochemical observations that can be directly associated with KH billow-induced turbulence are rare, primarily owing to their intermittent nature (De Silva et al., 1996).

This study aimed to explain how the fluxes of nutrients are affected by the Kuroshio-seamount interaction, specifically, the effects of variable KH billow-induced turbulence on vertical nitrate fluxes over a seamount. To help characterize the hydrodynamic conditions and identify possible KH instabilities, and determine how they affect nutrient distribution, conductivity-temperature-depth (CTD) profiling, water sampling (nitrate and Chl *a*), and echo sounder measurements were employed on the seamount that lies northeast of Green Island (henceforth referred to as the "K seamount"; **Figure 1A**). The results are not only helpful to better understand KH billow effect on pelagic ecosystems, but also useful for future biological investigations looking to understand and integrate seamount ecology.

MATERIALS AND METHODS

Sampling Stations and Physical Parameters

The target position, the summit of the K seamount, was located at 22.78°N, 121.44°E (**Figure 1A**). Two cruises to evaluate the physico-chemical and biological effects of billows were conducted around the K seamount, the first in May 2016 (small billow case, SBC) and the second in November 2018 (large billow case, LBC), on board the *R/V Ocean Researcher III* and *R/V Ocean Researcher I*, respectively. The definitions of SBC and LBC are further explained in the next section. Five sampling stations, namely K1–K5, were surveyed around the K seamount. The K2 station was located at the seamount summit, where strong KH billows had been previously observed (**Figure 1A**; Chang et al., 2016). The response of the pelagic ecosystem (i.e., nutrients and Chl *a*) to the variability of KH billows was addressed with a 24-h time series survey at K2 station over the seamount during both cruises. A total of six deployments were done on the K2 station, and each deployment was referred to as a cast, abbreviated as follows: SK2C1 to SK2C6 for SBC (i.e., May 2016) and LK2C1 to LK2C6 for LBC (i.e., November 2018). The other sampling stations (i.e., K1, K3, K4, and K5), which were placed 2–6 km from each side of K2 station to form the along-stream and cross-stream transects, were also surveyed to represent background conditions (station codes: SK1, SK3, SK4, and SK5 for the SBC, and LK1, LK3, LK4, and LK5 for the LBC) (**Figure 1A**).

Geostrophic current velocities derived from satellite altimeter data were retrieved from the Copernicus Marine Environment Monitoring Service[1] to map the Kuroshio's flow pattern. A shipboard, 120 kHz echo sounder (Simrad EK60) measured acoustic backscatter, capturing the microscale temperature variations generated by turbulence (**Figures 1B,C**). Temperature and density profiles were measured using an SBE 911 plus CTD (Seabird Electronics Inc., United States) down to 200 m. The mixed layer depth (MLD) was also estimated using the density threshold value of 0.03 kg m^{-3} (de Boyer Montégut et al., 2004). The euphotic zone depth (Z_E) is the depth where photosynthetically available radiation (PAR) is 1% of the value at the surface (Lee et al., 2007). The PAR profiles were estimated at each sampling station using a PAR irradiance meter (Chelsea Instruments Ltd.) attached to the CTD. Unfortunately, PAR profiles were only available during the SBC, and were not measured during the LBC. The dataset used in this study can be accessed in http://dx.doi.org/10.17632/23jzxbnknf.1 (Acabado, 2020).

Nitrate and Chlorophyll *a* Analysis

Seawater for nitrate and Chl *a* analyses was sampled at six depths, 5, 30, 60, 90, 120, and 150 m, using Teflon-coated Go-Flo bottles (20 L, General Oceanics Inc., United States) mounted

[1]https://marine.copernicus.eu/

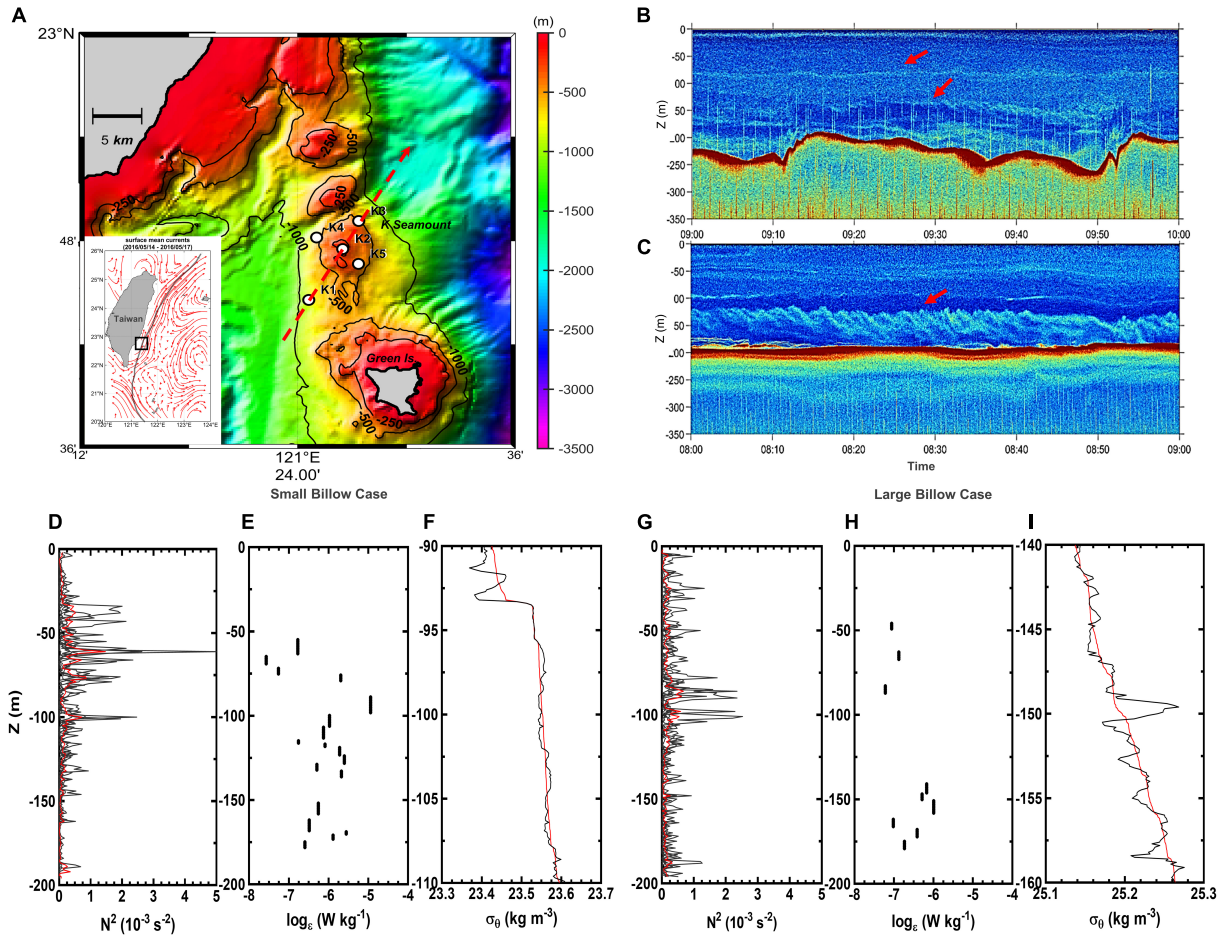

FIGURE 1 | The K seamount located north of Green Island off the southeastern coast of Taiwan **(A)**. The bathymetry shows isobaths (black contour lines) at –250, –500, and –1000 m depths. The white circles indicate the locations of the sampling stations on and around the K seamount. The red, dashed line is an along-stream transect indicating the direction and estimated location of the Kuroshio core. Examples of echosounder images (1-h duration) on K2 station during **(B)** small billow case (SBC; 2016) and **(C)** large billow case (LBC; 2018) show trains of billows (red arrows). The averaged values of the buoyancy frequency (N^2; red curves) were computed from the six CTD profiles measured on K2 station (black curves) during SBC **(D)** and LBC **(G)**. The water column profile matching the echo sounder images **(B,C)** showed active vertical overturning **(E,H)** with variable turbulent kinetic energy (TKE) dissipation rates (ε). The expanded observed [$\rho(z)$; black] and re-ordered [$\rho(z)$; red] density profiles **(F,I)** coincided with identified "well-mixed" patches **(E,H)**. Note the scale differences in *x*- and *y*-axes in **(F,I)**.

on a General Oceanics rosette assembly. Water samples for dissolved inorganic nutrient analysis were stored in 100 ml polyethylene bottles, immediately frozen in liquid nitrogen, and stored at −20°C until further analysis (Chen et al., 2017). Nitrate concentration (detection limit: 0.3 μM) was analyzed using the azo dye method, and measured spectrophotometrically (Metertech Inc., Taipei, Taiwan) using a custom-made flow injection analyzer (Knap et al., 1997; Gong et al., 2003). Nitrate profiles were generated from the empirical function between measured nitrate concentrations and temperature (2016: $r^2 = 0.89$, $p < 0.05$, $N = 99$; 2018: $r^2 = 0.80$, $p < 0.05$, $N = 60$).

For *in situ* Chl *a*, 2 L water samples were filtered through GF/F filter papers (Whatman, 47 mm) which were then frozen at −4°C until processing. The Chl *a* retained on the GF/F filters was extracted in 90% ethanol and measured using a fluorescence spectrophotometer (Turner Design 700, Turner Designs, United States). To generate a vertical profile, fluorescence was measured using a fluorescent probe (AQUATRACKA III, Chelsea Instruments Ltd., Untied Kingdom) attached to the CTD, which was calibrated using in situ Chl *a* (2016: $r^2 = 0.83$, $p < 0.001$, $N = 27$; 2018: $r^2 = 0.84$, $p < 0.001$, $N = 30$).

Estimation of Turbulent Kinetic Energy (ε), Eddy Diffusivity (K_ρ), and Vertical Nitrate Flux (F_{NO3})

To calculate ε, the Thorpe scale (L_T) was used to measure the vertical scale of the overturn, this scale is commonly used to quantify the magnitude of turbulence (Thorpe, 1977). Examples of estimations for the SBC and LBC are shown in **Figures 1E,F** and **H,I**, respectively. The Thorpe scale (L_T) is defined as the root mean square of Thorpe displacement (d), and expressed as:

$$L_T = [(\bar{d}^{\,2})]^{1/2}, \quad (1)$$

where d is the required vertical displacement of each data point within an overturn region from a reordered (stable) density profile $\rho(z)$ (red line) to an observed (unstable) density profile $\rho(z)$ (black line) (**Figures 1F,I**; Thorpe, 1977; Galbraith and Kelley, 1996). Finally, the turbulent kinetic energy (TKE) dissipation rate is expressed as:

$$\varepsilon = a^2 N^3 L_T^2, \quad (2)$$

where N is the buoyancy frequency and a is the ratio between the Ozmidov and Thorpe scales, set at $a = 0.8$ (Dillon, 1982; Finnigan et al., 2002; Chang et al., 2013). The resulting ε values are also shown in **Figures 1E,H**.

To calculate the nitrate flux within the water column, the eddy diffusivity (K_ρ) profile at each cast was computed using the TKE dissipation rates (ε) and the square of the buoyancy frequencies (N^2) as follows:

$$K_\rho = \Gamma\varepsilon/N^2, \quad (3)$$

where $\Gamma = 0.2$ is an estimate of the mixing efficiency (Osborn, 1980). To minimize CTD sensor noise effects, calibrated nitrate concentrations and eddy diffusivities were bin averaged over 10-m depth intervals, and were used to compute the upward nitrate flux as follows:

$$F_{NO3} = -K\rho\,(\delta NO_3/\delta z), \quad (4)$$

where F_{NO3} is the nitrate vertical diffusive flux, and $\delta NO_3/\delta z$ is the rate of change of nitrate concentration over depth. The vertical difference of F_{NO3} was computed from the mean of the nitrate fluxes at every 10-m depth interval from all K2 casts as follows:

$$(\Delta F_{NO3}) = \left(F_{NO3} \text{ in lower layer}\right) - \left(F_{NO3} \text{ in upper layer}\right), \quad (5)$$

where positive values of ΔF_{NO3} indicate convergence and effective vertical transport of nitrate (Tanaka et al., 2019). Overall, the estimation of ΔF_{NO3} provided direct indication of nitrate accumulation (positive value) and drain (negative value) associating KH billow-induced turbulence with vertical mixing over a seamount.

RESULTS

Oceanographic Context and the Relationship Between Turbulent Kinetic Energy Dissipation Rates and Kelvin–Helmholtz Instabilities

The upstream current velocity was 1.3 m s^{-1} near the surface (20 m) and gently decreased to 0.6 m s^{-1} at 180 m in 2018 cruise (LBC; **Supplementary Figure 1**). The upstream current velocity measured in 2016 (SBC) cruise is ∼0.3 m s^{-1} weaker than that in 2018 (**Supplementary Figure 1**). Furthermore, measurements were done during the neap and spring tides during the SBC and LBC, respectively, which may have an implication to the Kuroshio's velocity. Another factor that influences the Kuroshio's velocity is the presence of mesoscale eddies. For this, the spatial flow patterns of the Kuroshio characterized by the satellite-derived velocities were used (**Figure 2**). The different flow patterns of the surface currents east of Taiwan during the two cruises revealed a cyclonic eddy and an anticyclonic eddy along the eastern flank of the Kuroshio during the 2016 and 2018 cruises, respectively (**Figure 2**). Because of the association between eddy flow direction and current strength, the 2016 and 2018 cruises could be expected to have weak and strong Kuroshio flows, respectively, which was confirmed by the field observations of the KH billows (**Figures 2A,B**).

The echo sounder backscattering reflects the physically driven density gradient and/or biological/sediment particles. KH billow intensities in this study, as revealed by echo sounder images, are discussed in reference to the billows' temporal characteristics and behavior during the sampling cruises. In the 2016 cruise, the backscatter layers corresponded to the overturning events observed from the density profiles that are commonly induced by KH billows (**Figure 1B** and **Supplementary Figure 2**). The billows appeared small, relatively disorganized, and irregularly distributed, and were referred to as the SBC for the purposes of this study (**Figure 1B**). Two obvious billow-like signatures were detected, which propagated during SK2C3 and lasted through SK2C4, but had completely disappeared before SK2C5 (**Figure 1B** and **Supplementary Figure 3**). In contrast, during the 2018 cruise, a train of large KH billows approximately 50 m in amplitude was clearly distinguishable, and was thus referred to as the LBC (**Figure 1C**). The large billows were continuously observed from their near-summit onset on LK2C2 until LK2C6 (**Supplementary Figure 4**).

Vertical density overturns, identified by comparing the reordered and observed density profiles, were frequent in the sampling profiles (**Figures 1F,I**). During observations of the small and LBCs, the depth ranges with high TKE dissipation rates, ε, as inferred from the overturns, were generally consistent with the locations of the KH billows shown in the echo sounder images (**Figures 1B,C,E,H**). The value of ε ranged between O (10^{-7} to 10^{-6}) W kg^{-1} in the 50–180 m depths of the SK2C4 profile, as well as in the mixed patch between 140 and 180 m water depth in LK2C4 (**Figures 1B,C,E,H**). Overall, these "well-mixed" patches encompassed the KH billow layers in both sampling periods (**Figures 1F,I**).

Vertical Profiles of Variables on the K Seamount

During the SBC, the surface water was relatively warm (29°C), in contrast to LBC which was substantially cooler, dipping as low as 27°C (**Figures 3A,B**). The isotherms in LBC were perturbed at depths which coincided with the upper periphery of the KH billows (∼120 m) from LK2C2 to LK2C5 (**Figure 3B** and **Supplementary Figure 4**). Similarly, perturbed isotherms were observed between the two KH billows in the SBC (100–130 m; **Figure 3A** and **Supplementary Figure 3**). Isothermal doming signals were not detected from the water column above 200 m

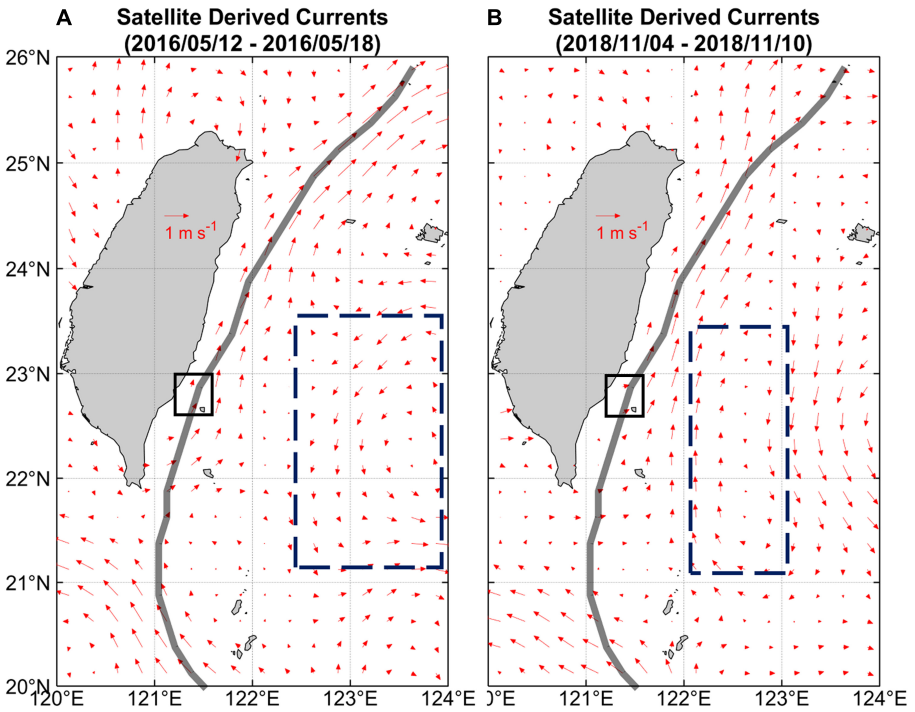

FIGURE 2 | Flow patterns of geostrophic currents (red arrows) during surveys in May 2016 **(A)** and November 2018 **(B)**. The axis of Kuroshio was close to the coast of Taiwan in both surveys and was directly flowing along the K seamount (black box). In 2016, the Kuroshio intrusion into the South China Sea followed a looping path and a cyclonic eddy existed to the east of the Kuroshio. In 2018, an anti-cyclonic eddy existed to the east of the Kuroshio, which could be expected to add to the current velocity. These eddies are highlighted along the east of the Kuroshio by boxes with dashed lines.

in the surveyed transects (**Figures 4A,B**, **5A,B**). An uplift of the 16.5°C isotherm was observed in the deepest sampling depth of LK5 (LBC) in the cross-stream transect, which seems to be a very weak upwelling signature (**Figure 5B**). Uplifting of isotherms was also evident in the leeward (toward SK3 and LK3) side of the seamount, which may be hydraulic jumps caused by the impeding seamount (**Figures 4A,B**). Generally, nitrate was measurable at shallower depths (40 m) with the 1.5 mmol m^{-3} isoline near the surface in the LBC, but undetected down to 65 m water depth in the SBC (**Figures 3C,D**, **4C,D**, **5C,D**). As for the Z_E, it was approximately at 101.5 ± 11.1 m depth on the K seamount during the SBC, but no data for the LBC.

Diel variation was not observed in the vertical distributions of Chl *a* (**Figures 3E,F**). The average concentration at the subsurface chlorophyll maximum (SCM) layer ranged between 0.33 and 0.35 μg L^{-1} at different layers in the water column between sampling periods. A moderately thick SCM layer was observed between 45 and 90 m water depth over K2 in the SBC, which overlapped with the shallower thin billow, and was maintained throughout the time-series survey (**Figure 3E** and **Supplementary Figure 3**). On the other hand, the SCM layer at K2 in the LBC was near the surface, between 10 and 45 m water depth, where turbulence was generally absent (**Figure 3F** and **Supplementary Figure 4**). However, the thick SCM layer in LK2C1 was not maintained, with a sudden drop in Chl *a* concentration at LK2C2 (**Figures 3F**, **4F**, **5F** and **Supplementary Figures 5A,B**). Both SCM layers were positioned just above the high nitrate concentration layer, following the 1.5 mmol m^{-3} isoline (**Figures 3C–F**, **4C–F**, **5C–F**).

Kelvin–Helmholtz Billow-Induced Turbulence and Vertical Nitrate Fluxes

The isopycnal range for Kuroshio in this region is from 21.5 to 25.7 σ_θ, and the temperature-salinity (T-S) curves were within the range for Kuroshio (**Figure 6**). Nitrate concentration in the water column ranged from 0.0 to 7.7 mmol m^{-3} and was undetectable above 65 m water depth in the SBC, which contrasted with the slightly higher concentrations during the LBC (1.1–7.6 mmol m^{-3}; **Figures 7D,I**). In addition, nitrate concentrations were significantly related to σ_θ (both r^2 = 0.9; $p < 0.05$), and the nitrate concentrations plotted against T-S plots revealed that the water column during the LBC featured higher concentrations of nitrates, especially in the shallower isopycnals than in the SBC (**Figure 6** and **Supplementary Figure 6**). At the same time, the nitrate concentration and salinity varied greatly with time and along the isopycnal direction within the range σ_θ = 23.5–25.0 at the six K2 sampling stations measured during the LBC time-series survey (**Figures 3D**, **6B**). The temporal change of nitrate concentrations along the isopycnals exhibited an increasing trend, suggesting that diapycnal upward nitrate injections occurred during the LBC time-series survey. For example, following the 3.5 mmol m^{-3} nitrate's isoline, which coincides with the 22.5 isotherm (or

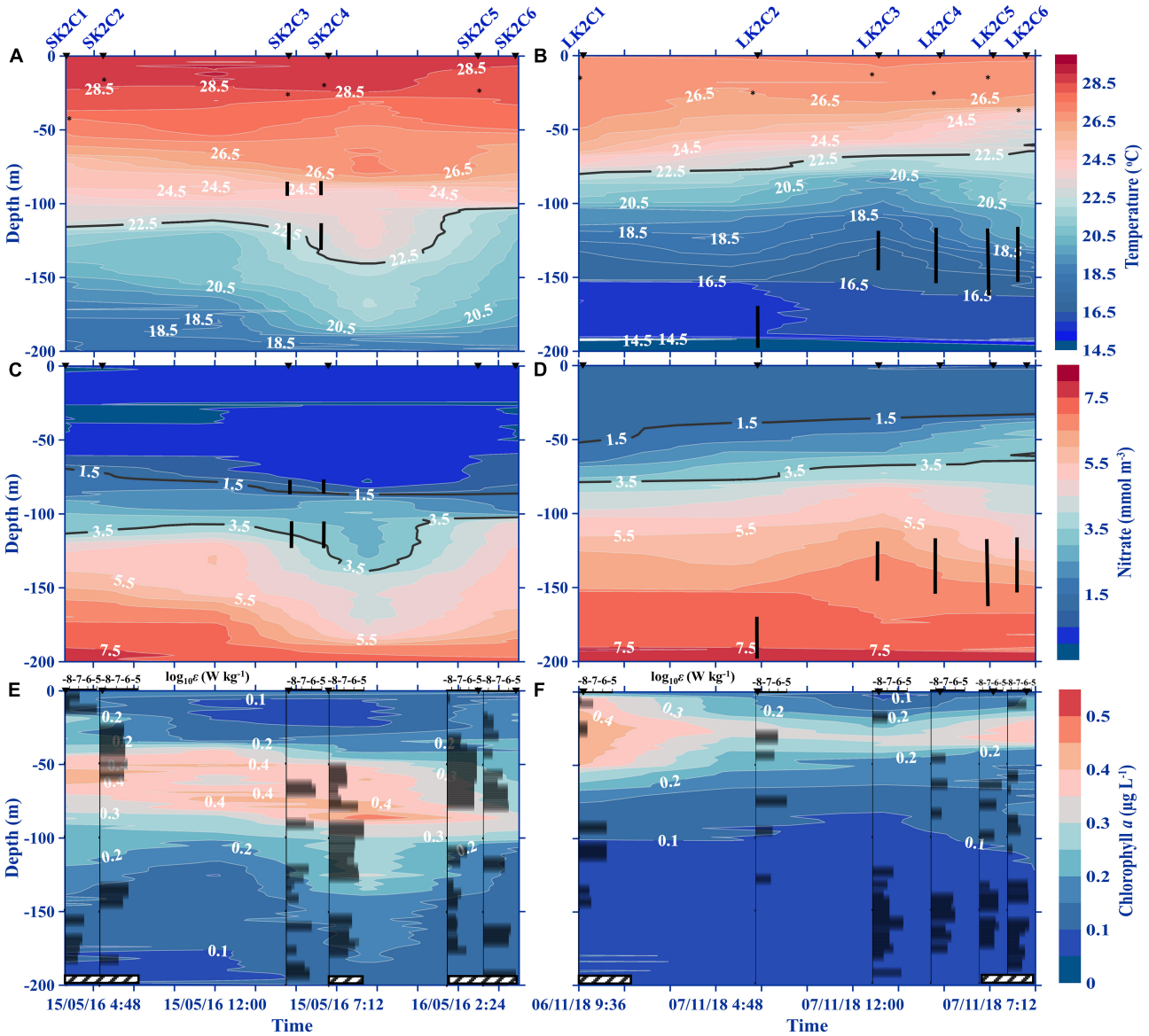

FIGURE 3 | Time-series depth contours of temperature **(A,B)**, nitrate **(C,D)**, and Chl *a* **(E,F)** during the SBC (2016; left panels) and the LBC (2018; right panels) at station K2. The cast and station numbers denoted above the top graph apply to all panels below. Asterisks on the temperature panels denote the mixed layer depths. The black vertical lines on **(A–D)** indicate KH billow depths in periods where they appeared. The black contour lines illustrating isotherms and nitrate isolines correspond to those discussed in the text **(A–D)**. The black bars on the chlorophyll profiles represent the TKE dissipation rates [$\log_{10}$ ε (W kg^{-1})]. Hatched bars along the *x*-axis indicate nighttime collections.

$\sigma_\theta \approx 23.5$), an increasing trend in nitrate concentration was observed through time (**Figures 3B,D**, **6B**). The strong turbulent mixing in the LBC occurred between 80 and 140 m water depth in all time-series sampling stations, which overlapped the upper braids of the KH billows coinciding with this density range, consistent with the above interpretation. In contrast, the T-S diagram for the SBC's K2 sampling stations revealed relatively small temporal variabilities in nitrate concentrations and salinity with a range 34.9–35.0 within the 23.5–24.0 σ_θ (**Figure 6A**). The mixing process reached almost 50 m water depth in the LBC, but the mixing signal was weak in the SBC with undetected nitrate concentration near the surface (**Figure 6**).

As for the eddy diffusivity, it was in the range of K_ρ = O (10^{-6} to 10^{-3}) m^2 s^{-1}, and was generally stronger within the nitracline and billow depths. Furthermore, they also appeared to have a stronger nitrate gradient [($\delta NO_3/\delta z$) = O (10^{-2} to 10^{-1}) mmol m^{-4}] than the gradients outside of these depth ranges (**Figures 7A,B,F,G**). The billow layers (80–90 and 120–140 m) in the SBC had eddy diffusivities of O (10^{-4}) and O (10^{-3}) m^2 s^{-1},

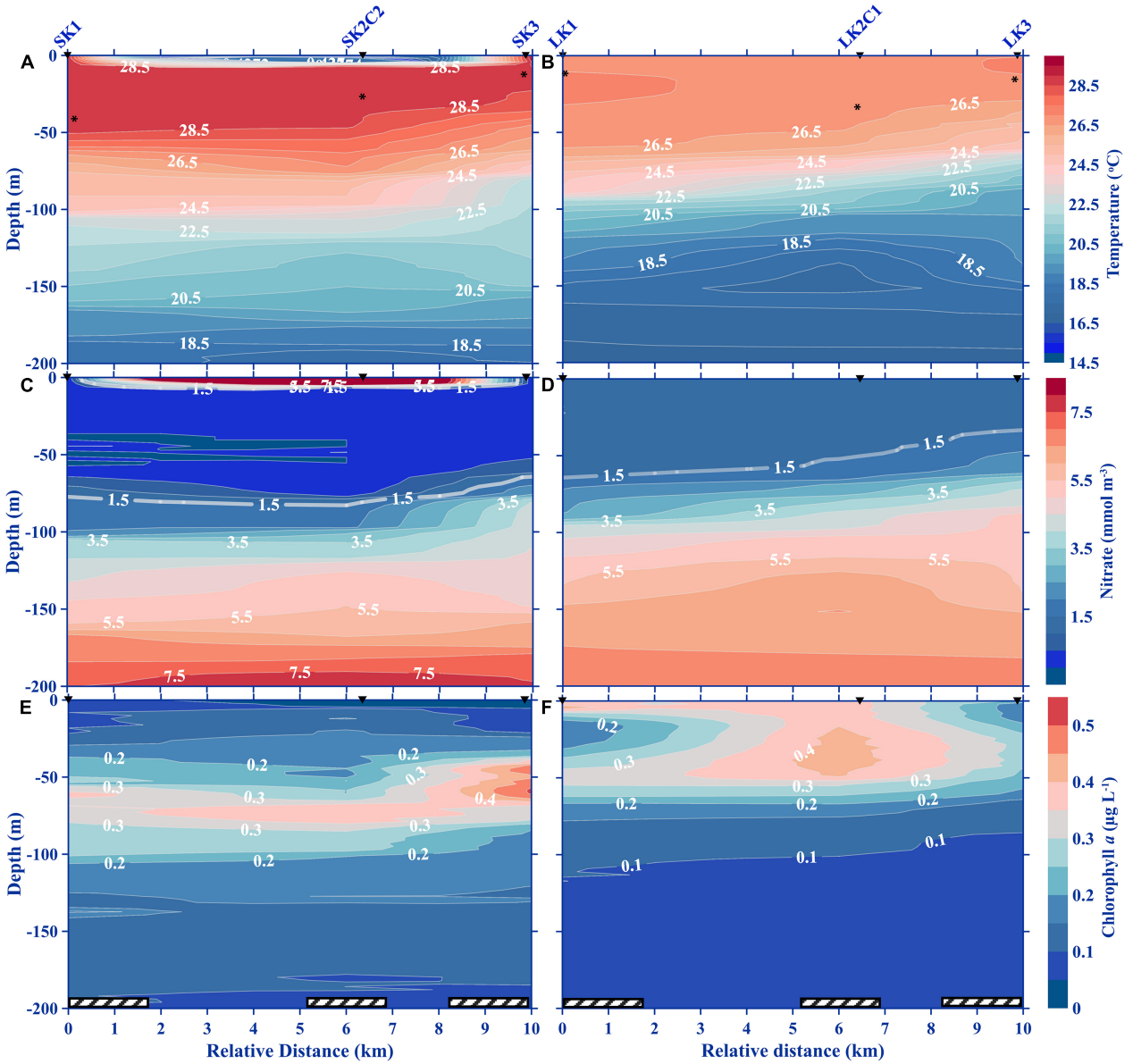

FIGURE 4 | Vertical profiles of temperature **(A,B)**, nitrate **(C,D)**, and Chl *a* **(E,F)** in the along-stream transect during small (2016) and large (2018) billow cases. The cast and station numbers denoted above the top graph apply to all panels in the column. Asterisks on the temperature panels denote the mixed layer depths. Hatched bars along the *x*-axis indicate nighttime collections.

with the larger diffusivity detected in the shallower billow layer (**Figures 7A,E**). At the billow depth of 120–160 m in the LBC, K_ρ = O (10^{-3}) m^2 s^{-1} was comparable to that in the SBC's shallow billow (**Figures 7F,J**).

The averaged F_{NO3} over the water column (0–200 m) at K2 station were 1.1 and 1.5 mmol m^{-2} day^{-1} in the SBC and LBC, respectively. The estimated nitrate flux in the water column during the SBC ranged from 0.0 to 4.7 mmol m^{-2} day^{-1}, with higher values recorded in the shallow billow layer (**Figures 7C,E**). On the other hand, the LBC recorded an estimated nitrate flux ranging from 0.0 to 10.0 mmol m^{-2} day^{-1}, which appeared to be larger within the billow depths. The calculated ΔF_{NO3}, particularly in the billow regions, were 2.1 and 5.2 mmol m^{-2} day^{-1} in the SBC and LBC, respectively.

DISCUSSION

Hydrographic Conditions and Response to Variable Kelvin–Helmholtz Billow Intensities Over Time

This study presented two mechanisms, such as mesoscale eddies and tide to modulate the Kuroshio's velocity and the intensity

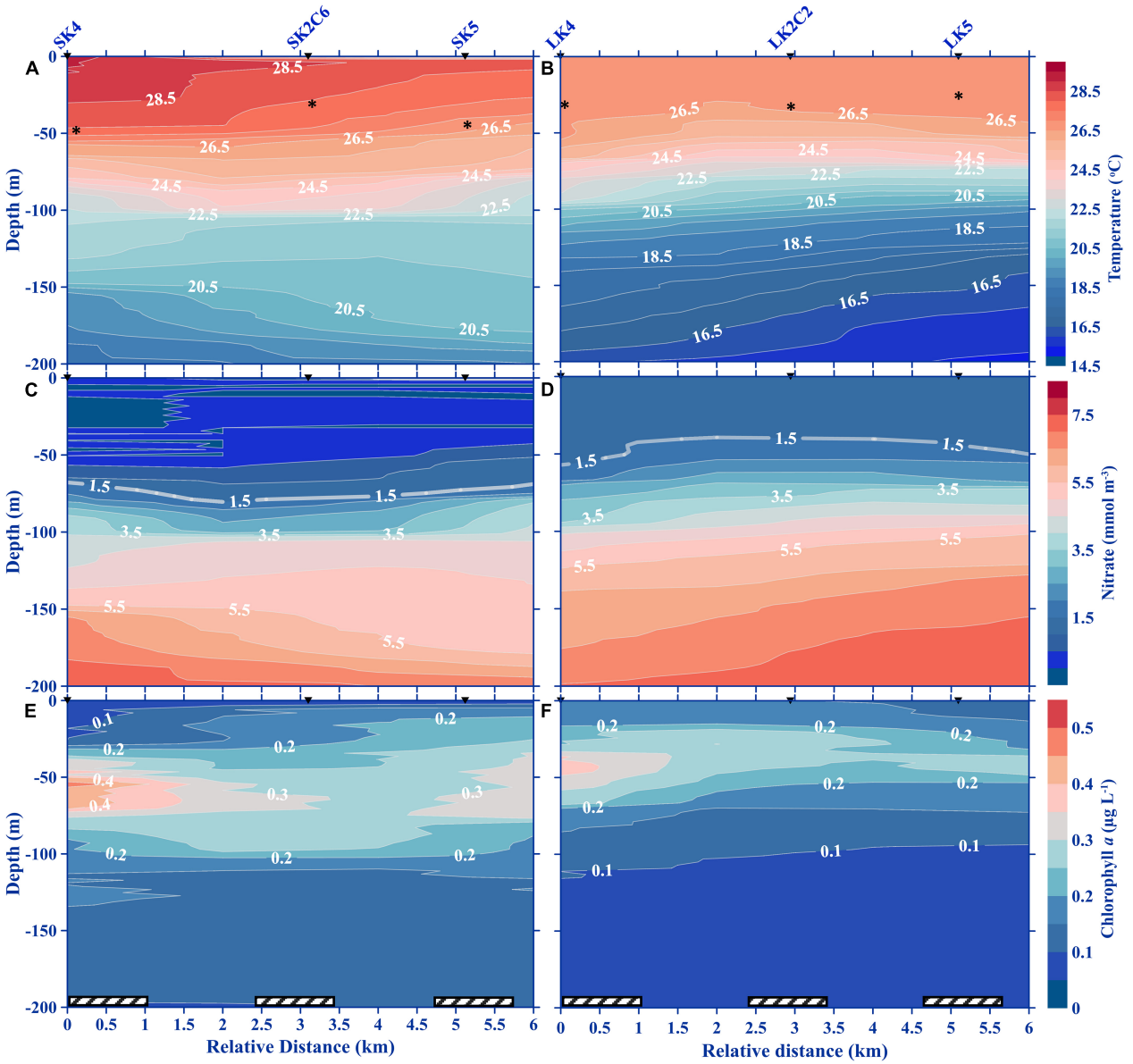

FIGURE 5 | Vertical profiles of temperature **(A,B)**, nitrate **(C,D)**, and Chl *a* **(E,F)** in the cross-stream transect during small (2016) and large (2018) billow conditions. The cast and station numbers denoted above the top graph apply to all panels in the column. Asterisks on the temperature panels denote the mixed layer depths. Hatched bars along the *x*-axis indicate nighttime collections.

of the associated KH billows. The upstream current velocity of the Kuroshio was approximately 0.3 m s^{-1} weaker during the SBC than during the LBC (**Supplementary Figure 1**). The different upstream conditions were presumably related to the tides during the experiments. Strong tidal currents associated with the spring tide may have further enhanced the Kuroshio's velocity during the LBC, eventually resulting in larger KH billows (Du et al., 2008). In describing the Kuroshio's velocity, the satellite derived geostrophic flow patterns, observed as cyclonic and anticyclonic eddies, were also instrumental. This was because when cyclonic and anticyclonic eddies encounter the Kuroshio, they reduce and enhance poleward transport which characterized the SBC and LBC in this study, respectively (Jan et al., 2015; Tsai et al., 2015; Chang et al., 2018). On the other hand, the presence of the KH billows have been demonstrated to be an S-shaped echo band, similar to this study (Geyer et al., 2010; Chang et al., 2016; Hasegawa et al., 2021). In describing the KH billows, their transitory nature was observed during the time-series surveys. The overturning layers, which are commonly induced by KH billows, matched the backscatter features on the echo sounder images (**Figures 1B,C,F,I** and **Supplementary Figure 2**; Smyth and Moum, 2000). The billows during the SBC were small and intermittent while the large billows during the LBC were 50 m in height, clearly apparent, and persisted for

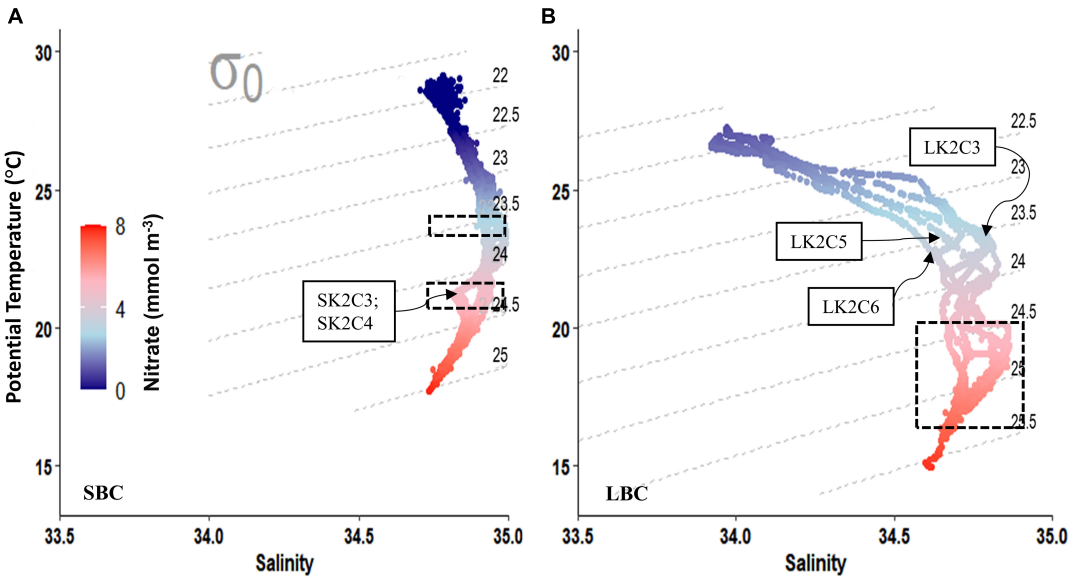

FIGURE 6 | Color coded nitrate concentrations were plotted on a temperature-salinity diagram to show different relationships of nitrates with isopycnals, σ_θ (kg m^{-3}) during **(A)** small billow case (SBC) and **(B)** large billow case (LBC). Dashed boxes highlight the nitrate profile in the approximate locations of KH billows. The profiles of the K2 sampling stations where billows occurred during the SBC were labeled in **(A)**. Since KH billows were observed throughout the time-series survey during the LBC, the temporal order of the profiles was indicated by a few sampling station labels in **(B)**. Isopycnal labels are on the left-hand side of each panel.

more than 12 h (**Figures 1B,C** and **Supplementary Figures 3**, **4**). Furthermore, in the LBC, the abrupt along-isopycnal shifts of the nitrate concentrations between profiles in the time-series survey within the density range, σ_θ = 23.0–25.0 were interpreted as strong diapycnal mixing signals, which were likely dominated by KH billow-induced turbulence (**Figures 3D**, **6B**). In addition, the buoyancy frequency could also have an impact on the billow size (**Figures 1D,G**). This can be evaluated by computing the Ozmidov scale, $L_0 = \sqrt{\varepsilon/N^3}$, although, it needs a direct measurement of TKE dissipation rate, which is not available in the present study.

To examine KH instabilities in detail, the calculated Richardson number (*Ri*) was <0.25 within the billow layers, which is the critical value indicating the threshold for billow formation (**Supplementary Figure 7**; Howard, 1961; Miles, 1961; Chang, 2021). It must be noted that Chang et al. (2016) recorded TKE values of O (10^{-4} to 10^{-3}) W kg^{-1} at the billow cores on the K seamount, which were sufficient to encourage mixing with adjacent water bodies. In this study, TKE dissipation rates were weaker, at O (10^{-7} to 10^{-6}) W kg^{-1}, but appeared to be stronger nearer the billows. Turbulence can be a vital contributor to ecosystem function, serving a variety of roles. One notable role is the resuspension and transport of nutrients from deeper into shallower water, as similarly observed by Shroyer (2012). Though turbulence created *via* KH instabilities is relatively small-scale, the resulting diffusive energy can be significant. This study measured eddy diffusivities on the seamount ranging from O (10^{-6} to 10^{-3}) m^2 s^{-1}, weaker but still comparable to those reported in the downstream Kuroshio, which were sufficiently influential to enrich downstream nutrient levels (Nagai et al., 2019b; Tanaka et al., 2019; Kobari et al., 2020). Furthermore, Guo et al. (2013) reported that local changes in nitrate concentration in shallower depths (i.e., on seamounts) contribute significantly to the downstream increase in nitrate concentration along the Kuroshio. These measurements demonstrated the potential role of KH billows on seamounts in the biogeochemical enhancements from the upstream Kuroshio.

Importance of Kelvin–Helmholtz Billows as a Driver for Vertical Nitrate Flux in the Kuroshio

Turbulence-induced nitrate flux in both billow conditions were of the same magnitude, and were observed to mix large amounts of nutrients from the deep water to the Z_E ($\approx$ 101.5 $\pm$ 11.1 m) (**Figures 7C,H**). In the case of the SBC, the uplifted nutrient-rich water partially overlapped with the deep, thicker billow train and reached the shallower billow (**Figure 7E**). Billows have been observed to trap fluids from other water parcels, so it is likely that the nutrients transported from deeper water were entrained in the shallower billows, sustaining thin chlorophyll patches near the surface (**Figures 3E**, **7E**; Woods and Wiley, 1972). The F_{NO3} in this billow layer suggested that shallow billows, regardless of vertical thickness, can entrain ambient dissolved inorganic nutrients in the euphotic zone (**Figures 7B,C**). In addition, greater irradiance in the shallow layer could reinforce elevated biological production. The enriched patch of Chl *a* above the seamount could attract predators such as zooplankton and ultimately become a hotspot for aggregations of nektonic stocks (Sibert et al., 2000; Morato et al., 2008).

The ΔF_{NO3} during the LBC (5.2 mmol m^{-2} day^{-1}) revealed that the large amplitude and persistent KH billows were 40%

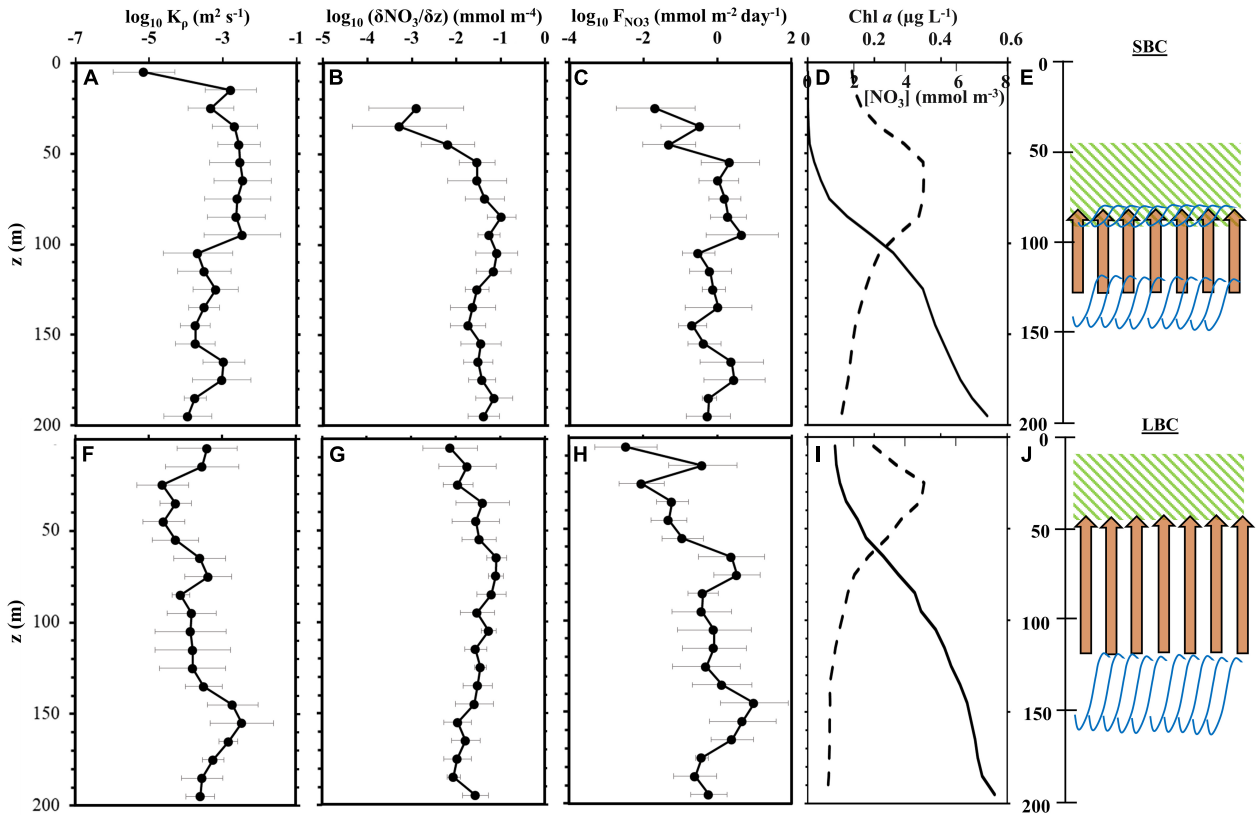

FIGURE 7 | The top (SBC) and bottom (LBC) rows include vertical profiles of environmental parameters on the K seamount. Profiles of eddy diffusivity, K_ρ **(A,F)**, nitrate gradient **(B,G)**, and vertical nitrate flux, F_{NO3} **(C,H)** from all casts deployed on K2 station are shown. Gray solid lines are relative standard deviations. The vertical profiles of averaged Chl *a* (dashed line; upper top axis label) and nitrate (solid line; lower top axis label) concentrations are shown **(D,I)**. Schematic of the approximate locations of nutrient uplift (the starting point of the orange arrows indicate the depth where abrupt changes in the nitrate isolines were observed based on **Figures 3C,D**; the arrowheads mark the 1.5 mmol m^{-3} nitrate isoline), KH billows (blue curved lines), and subsurface chlorophyll maximum (SCM; green hatched box) within the water column during the SBC (**E**; two billow layers) and LBC **(J)**. Based on the time-series sampling at station K2 where KH billows were observed (**Figure 3** and **Supplementary Figures 3**, **4**).

more effective in vertically transporting nitrates than the thin and transitory billows of the SBC. This suggested that, when strong turbulence occurs near the summit, it may be more effective in stirring up nutrient-rich water from deeper to shallower water (Shroyer, 2012). Although the supply depth overlaps only the base of the euphotic zone, the substantially cooler water column during the LBC may have rendered the upward nitrate flux more effective in reaching the mixed layer (Zhang et al., 2016). In addition, the overall eddy diffusivity in the LBC was one order of magnitude weaker [O (10^{-4} m^2 s^{-1})] than in the SBC (**Figures 7A,F**). However, it may be expected that large diffusivity, which coincides with cooler temperature and large nutrient vertical gradient may induce a more efficient vertical nitrate flux, stimulating an increase in phytoplankton biomass (using Chl *a* as a proxy). Furthermore, the high nutrient layers in both the SBC and LBC were located at the base of SCM layers (**Figures 3C–F**, **7E,J**). Thus, an increase in phytoplankton biomass was likely related to the nitrate flux resulting from the turbulence produced by KH billows, though, shallower billows may have a more direct influence to the productivity near the surface. This evidence augments our understanding of seamount as "hotspots" of nutrient supply in an otherwise impoverished and nutrient-poor environment.

Impact of Kelvin–Helmholtz Billow-Induced Vertical Nitrate Flux to the Oligotrophic Kuroshio's Enhanced Productivity

Flow-seamount interactions have received so much attention over the past several decades that most mesoscale physical features are already well studied and understood (Boehlert, 1988; Mohn and Beckmann, 2002; Chang et al., 2016). Taking advantage of this, data from past transects positioned laterally from the Taiwan coast toward the Pacific were analyzed to obtain a broader view of the upstream Kuroshio (**Supplementary Figure 8**). A continuous band of Chl *a* up to 0.4 μg L^{-1} between 40 and 70 m depth in KTV3 transect demonstrated the upstream Kuroshio's productivity, which could be potentially advected downstream (**Supplementary Figures 8A,B**). In KTV2 transect, two well-defined productive systems were identified by strong SCM layers: the enriched coastal system and the seamount

system, located immediately upstream of the K seamount (**Supplementary Figures 8A,C**). This lateral difference in Chl *a* concentration across KTV2 provided substantial evidence that special conditions related to nutrient cycling and production may exist on the K seamount.

In this study, the Chl *a* concentrations on the K seamount were varied throughout the surveys (**Figures 3E,F**). There was evidence of possible trapping of allochthonous Chl *a* on the seamount, especially during LBC (**Figures 3F**, **4F**), similar to the observations by Genin and Boehlert (1985). Satellite images of surface Chl *a* did not show significant horizontal advection of Chl *a* toward the K seamount (**Supplementary Figure 9**). However, assuming that Kuroshio's horizontal flow speed (U) ranges between 1.0 and 1.5 m s^{-1} and the K seamount's horizontal length scale (L) is 5 km, the residency time (L/U) of Chl *a* on the summit would only be between 0.9 and 1.4 h (Chang et al., 2016). The Kuroshio's flow speed may then play a significant role in the retention time, as well as the downstream transport, of the locally produced phytoplankton biomass on the seamount. For instance, the SCM layer was thick and consistent when the Kuroshio Current was weak, in contrast to the highly variable SCM layer when its current was stronger (**Figures 3E,F**).

Despite being oligotrophic, the Kuroshio has exhibited an evolution in its chemical characteristics going downstream (**Table 1**; Chen et al., 2017; Saito, 2019). This has been demonstrated in the earlier observations along the northeast Taiwan coast where lateral F_{NO3} was 5.0–9.0 mmol m^{-2} day^{-1} (**Table 1**; Chen et al., 2017). Furthermore, direct upward nitrate flux measurements along the Kuroshio have shown potential influence to the elevation of nitrate concentrations along the Kuroshio's nutrient stream. A vertical nitrate flux of 4.7 mmol m^{-2} day^{-1} was recorded in the Luzon Strait along the Kuroshio path, and was expected to be transported downstream along the eastern coast of Taiwan (Tsutsumi et al., 2020). Furthermore, an upward nitrate flux of 1.0 mmol m^{-2} day^{-1} was estimated along the Tokara Strait in the Kuroshio (Kobari et al., 2020). This upward nutrient supply was suggested to be important in enhancing the biological production as the Kuroshio flows along the coastal margins of Japan (Nagai et al., 2019b; Kobari et al., 2020). The Kuroshio Extension front was previously found to exhibit a vertical nitrate flux of 0.1 mmol m^{-2} day^{-1} (Kaneko et al., 2013). Recent estimations revealed a one order of magnitude larger nitrate flux (1.0 mmol m^{-2} day^{-1}) in the Kuroshio Extension (Nagai et al., 2019a). The Izu Ridge displayed the largest magnitude of vertical nitrate flux (1.0–10.0 mmol m^{-2} day^{-1}) as the Kuroshio drew nitrates from the North Pacific Intermediate Water (Tanaka et al., 2019), which is similar to the results of this study. Furthermore, recent microstructure float data and nutrient measurements revealed that elevated nutrient flux extends up to 100 km downstream from the Izu Ridge (Nagai et al., 2021). Moreover, KH billows were observed to be persistent on the K seamount over a 6-month measurement period (Chang et al., 2016). Consequently, nitrate flux induced by KH billow may also persist for similarly extended durations, and can be potentially transported for long distances downstream of the Kuroshio. Since strong vertical nutrient flux induces rapid increases in phytoplankton biomass, a continuous flux of nutrients to the euphotic zone would promote primary production on the K seamount that could sustain aggregations of zooplankton and nektonic stocks (Kobari et al., 2020). However, information on larval fish and zooplankton biomass would be required to understand how grazing interacts with this biological productivity.

TABLE 1 | Estimates of nitrate flux (F_{NO3}) along the Kuroshio where strong vertical mixing occurs.

Location	F_{NO3} (mmol m^{-2} day^{-1})	References
K Seamount, Southeast Taiwan	0.0–10.0	This study
Kuroshio Extension front, northwest Pacific	0.1	Kaneko et al., 2013
	1.0	Nagai et al., 2019a
Northeast Taiwan	5.0–9.0	Chen et al., 2017
Izu Ridge, south of Japan	1.0–10.0	Tanaka et al., 2019
Tokara Strait, south of Japan	1.0	Kobari et al., 2020
Luzon Strait, north of Philippines	4.7	Tsutsumi et al., 2020

These studies include straits, ocean ridges, fronts, and seamounts. All the values in the table were upward nitrate fluxes, except for the lateral nitrate flux reported in Northeast Taiwan by Chen et al. (2017).

CONCLUSION

This study attempted to provide insight into the dominant physical processes that facilitate high productivity over seamounts, which are still poorly understood. Firstly, variability in the intensity of KH billows was revealed. The study examined two KH billow conditions over a seamount in the Kuroshio: (1) intermittent, SBC, and (2) persistent, LBC. The shallower KH billows, were more likely to sustain subsurface chlorophyll concentrations by transporting and entraining nutrients at the surface, however, their vertical scale was limited, which reduced access to deeper nutrients. The limited access to nitrates could impede phytoplankton growth, though small nutrient concentrations can be sufficient enough to support primary productivity. Chen et al. (2008) estimated that 30–50% of primary production can be sustained by nitrate-uptake-based new production, particularly in the Kuroshio. If the retention time of phytoplankton over the seamount is extended (i.e., SBC, weak Kuroshio velocity), there is the potential for efficient uptake of vertically mixed nutrients for increased phytoplankton biomass. In contrast, the deeper billows during the LBC were highly effective in supplying nutrients (ΔF_{NO3} = 5.2 mmol m^{-2} day^{-1}) directly from the deep water. Thus, the deep and persistent billow-induced turbulence promoted high nutrient supply (F_{NO3} = 0.0–10.0 mmol m^{-2} day^{-1}) from deep to subsurface water. However, the strong Kuroshio flow could sweep Chl *a* and nutrients to the lee.

Next, this study presents direct evidence relating KH billow-induced turbulence to vertical nitrate flux. The KH billows

identified in this study were triggered by $Ri < 0.25$ due to strong shears. Diffusive mechanisms, i.e., the KH billows, within the water column are known to supply nutrients from deeper water to the euphotic zone, especially in oligotrophic areas. The turbulence generated by KH billows on seamounts produced large diffusivities [K_ρ = O (10^{-4} to 10^{-3}) m^2 s^{-1}] wherein high nutrient fluxes are achieved, reaching water near the surface; the LBC displayed a 40% more efficient upward nitrate flux than the SBC. Furthermore, this study showed wide variability in the biophysical properties of a single seamount. The depths and locations of the instabilities and the intensity of the current velocity all influenced the nutrient supply around the seamount. Considering the numerous factors in play, there are a multitude of possible interactions that could create unique hydrographic phenomena at any given seamount. Thus, understanding the variability of the upward nitrate flux on the K seamount is instrumental in predicting local primary production and how much the seamount contributes to Kuroshio enrichment.

Lastly, the overall averaged F_{NO3} in the water column during the SBC and LBC (1.1 and 1.5 mmol m^{-2} day^{-1}, respectively) were one magnitude stronger than those reported in the oligotrophic east Atlantic, but similar to the estimates in the downstream Kuroshio. Thus, in addition to straits, fronts, and ridges, this study contributes to the understanding of the paradox of the Kuroshio (high production in an oligotrophic environment), where KH billows on shallow seamounts induce upward nitrate supply that can be transported downstream.

The deep-sea is considered one of the last great frontiers on Earth. This study provided insight into the phenomena that make seamounts oases of life in an oligotrophic ocean, revealing how variable KH billows drive nutrient supplies. Since the Kuroshio mostly flows over numerous abrupt seamounts, persistent turbulent mixing and strong vertical nutrient fluxes can be expected. Future research should include higher trophic levels from the pelagic ecosystem to estimate how KH billow-induced turbulence and diffusive nitrate fluxes benefit biological communities on seamounts and, how these communities respond to regularly disturbed nutrient sources.

DATA AVAILABILITY STATEMENT

The datasets presented in this study can be found in online repositories. The names of the repository/repositories and accession number(s) can be found below: Mendeley: http://dx.doi.org/10.17632/23jzxbnknf.1.

AUTHOR CONTRIBUTIONS

CA conducted the cruise surveys and laboratory processing, analyzed the data, wrote the manuscript, prepared the figures and table, and reviewed drafts of the manuscript. Y-HC, M-HC, and C-CC provided funding, guidance on data analysis, validation, and reviewed drafts of the manuscript. All authors contributed in the conceptualization of the study.

FUNDING

Funding for the cruises and experiments was supported by Taiwan's Ministry of Science and Technology (MOST) under grants MOST 105-2119-M-003-007-MY2, 107-2611-M-003-001-MY3, and 110-2611-M-003-002 to C-CC, MOST 108-2611-M-002-017 and 110-2611-M-002-002 to M-HC, and CWB of Taiwan project: 1062076C to Y-HC. This article was subsidized by National Taiwan Normal University (NTNU), Taiwan, ROC.

ACKNOWLEDGMENTS

We are grateful for the crew of *R/V Ocean Researcher I* and *III* for the cruise operations. Special thanks to Sen Jan who led the 2018 cruise, Chin-Zhou Yeh, Teresa Hsieh, Ting-Wei Chang, Chun-Yi Lu, and Val Wang for assisting in the experiments on board and in the laboratory, including echo sounder and CTD measurements and water sampling. We thank the MOST Ocean Data Bank (https://www.odb.ntu.edu.tw/en/) for providing bathymetry data used to plot **Figure 1A**. Comments from Ren-Chieh Lien were most helpful. Most of the laboratory experiments were done in Frank Shiah's Laboratory in Academia Sinica. We also thank the reviewers, Takeyoshi Nagai and Hiroaki Saito, for the rigorous and thorough evaluation of this manuscript.

SUPPLEMENTARY MATERIAL

The Supplementary Material for this article can be found online at: https://www.frontiersin.org/articles/10.3389/fmars.2021.680729/full#supplementary-material

REFERENCES

Acabado, C. (2020). *Kelvin-Helmholtz Billow Intensity Determines Effect on Pelagic Ecosystems in the Kuroshio*, 1 Edn. Taiwan: National Taiwan Normal University.

Barkley, R. A. (1970). The Kuroshio Current. *Sci. J.* 6, 54–60.

Biggs, B. J. F., and Thomsen, H. A. (1995). Disturbance in stream periphyton by perturbations in shear stress: time to structural failure and differences in community resistance. *J. Phycol.* 31, 233–241.

Blumen, W., Banta, R., Burns, S. P., Fritts, D. C., Newsom, R., Poulos, G. S., et al. (2001). Turbulence statistics of a Kelvin–Helmholtz billow event observed in the night-time boundary layer during the cooperative atmosphere–surface exchange study field program. *Dynam. Atmospher. Oceans* 34, 189–204. doi: 10.1016/S0377-0265(01)00067-7

Boehlert, G. W. (1988). Current-topography interactions at mid-ocean seamounts and the impact on pelagic ecosystems. *GeoJournal* 16, 45–52. doi: 10.1007/BF02626371

Boehlert, G. W., and Genin, A. (1987). A review of the effects of seamounts on biological processes *Seamounts, Islands and Atolls. Geophys. Monogr.* 43, 319–334.

Chang, M. H. (2021). Marginal Instability Within Internal Solitary Waves. *Geophys. Res. Lett.* 48:2021gl092616. doi: 10.1029/2021gl092616

Chang, M. H., Jan, S., Mensah, V., Andres, M., Rainville, L., Yang, Y. J., et al. (2018). Zonal migration and transport variations of the Kuroshio east of Taiwan induced by eddy impingements. *Deep Sea Res. Part I Oceanogr. Res. Pap.* 131, 1–15. doi: 10.1016/j.dsr.2017.11.006

Chang, M. H., Jheng, S. Y., and Lien, R. C. (2016). Trains of large Kelvin-Helmholtz billows observed in the Kuroshio above a seamount. *Geophys. Res. Lett.* 43, 8654–8661. doi: 10.1002/2016gl069462

Chang, M. H., Tang, T. Y., Ho, C. R., and Chao, S. Y. (2013). Kuroshio-induced wake in the lee of Green Island off Taiwan. *J. Geophys. Res. Oceans* 118, 1508–1519. doi: 10.1002/jgrc.20151

Chen, C. A., Huang, T. H., Wu, C. H., Yang, H., and Guo, X. (2021). Variability of the nutrient stream near Kuroshio's origin. *Sci. Rep.* 11:5080. doi: 10.1038/s41598-021-84420-5

Chen, C. C., Jan, S., Kuo, T. H., and Li, S. Y. (2017). Nutrient flux and transport by the Kuroshio east of Taiwan. *J. Mar. Syst.* 167, 43–54. doi: 10.1016/j.jmarsys.2016.11.004

Chen, Y. L., Chen, H. Y., Tuo, S. H., and Ohki, K. (2008). Seasonal dynamics of new production from Trichodesmium N2 fixation and nitrate uptake in the upstream Kuroshio and South China Sea basin. *Limnol. Oceanogr.* 53, 1705–1721.

Cheng, Y. H., Chang, M. H., Ko, D. S., Jan, S., Andres, M., Kirincich, A., et al. (2020). Submesoscale Eddy and Frontal Instabilities in the Kuroshio Interacting With a Cape South of Taiwan. *J. Geophys. Res. Oceans* 125:2020jc016123. doi: 10.1029/2020jc016123

de Boyer Montégut, C., Madec, G., Fischer, A., Lazar, A., and Iudicone, D. (2004). Mixed layer depth over the global ocean: An examination of profile data and a profile-based climatology. *J. Geophys. Res.* 109:2004jc002378. doi: 10.1029/2004jc002378

De Silva, I. P. D., Fernando, H. J. S., Eaton, F., and Hebert, D. (1996). Evolution of Kelvin-Helmholtz billows in nature and laboratory. *Earth Planet. Sci. Lett.* 143, 217–231. doi: 10.1016/0012-821X(96)00129-X

Dillon, T. M. (1982). Vertical overturns: A comparison of Thorpe and Ozmidov length scales. *J. Geophys. Res.* 87:JC087iC1209601. doi: 10.1029/JC087iC12p09601

Du, T., Tseng, Y.-H., and Yan, X.-H. (2008). Impacts of tidal currents and Kuroshio intrusion on the generation of nonlinear internal waves in Luzon Strait. *J. Geophys. Res.* 113:2007jc004294. doi: 10.1029/2007jc004294

Finnigan, T. D., Luther, D. S., and Lukas, R. (2002). Observations of enhanced diapycnal mixing near the Hawaiian Ridge. *J. Physic. Oceanogr.* 32, 2988–3002.

Galbraith, P. S., and Kelley, D. E. (1996). Identifying overturns in CTD profiles. *J. Atmosph. Oceanic Technol.* 13, 688–702.

Genin, A., and Boehlert, G. W. (1985). Dynamics of temperature and chlorophyll structures above a seamount: An oceanic experiment. *J. Mar. Res.* 43, 907–924. doi: 10.1357/002224085788453868

Geyer, W. R., Lavery, A. C., Scully, M. E., and Trowbridge, J. H. (2010). Mixing by shear instability at high reynolds number. *Geophys. Res. Lett.* 37:2010gl045272. doi: 10.1029/2010gl045272

Gong, G.-C., Wen, Y.-H., Wang, B.-W., and Liu, G.-J. (2003). Seasonal variation of chlorophyll a concentration, primary production and environmental conditions in the subtropical East China Sea. *Deep Sea Res. Part II Top. Stud. Oceanogr.* 50, 1219–1236. doi: 10.1016/s0967-0645(03)00019-5

Guo, X. Y., Zhu, X. H., Long, Y., and Huang, D. J. (2013). Spatial variations in the Kuroshio nutrient transport from the East China Sea to south of Japan. *Biogeosciences* 10, 6403–6417. doi: 10.5194/bg-10-6403-2013

Hasegawa, D., Matsuno, T., Tsutsumi, E., Senjyu, T., Endoh, T., Tanaka, T., et al. (2021). How a Small Reef in the Kuroshio Cultivates the Ocean. *Geophys. Res. Lett.* 48:2020gl092063. doi: 10.1029/2020gl092063

Hebert, D., Moum, J. N., Paulson, C. A., and Caldwell, D. R. (1992). Turbulence and internal waves at the equator. Part II: Details of a single event. *J. Phys. Oceanogr.* 22, 1346–1356.

Howard, L. N. (1961). Note on a paper of John W. Miles. *J. Fluid Mech.* 10, 509–512. doi: 10.1017/S0022112061000317

Jan, S., Yang, Y. J., Wang, J., Mensah, V., Kuo, T. H., Chiou, M. D., et al. (2015). Large variability of the Kuroshio at 23.75°N east of Taiwan. *J. Geophys. Res. Oceans* 120, 1825–1840. doi: 10.1002/2014jc010614

Kaneko, H., Yasuda, I., Komatsu, K., and Itoh, S. (2013). Observations of vertical turbulent nitrate flux across the Kuroshio. *Geophys. Res. Lett.* 40, 3123–3127. doi: 10.1002/grl.50613

Knap, A. H., Michaels, A. F., Steinberg, D. K., Bahr, F., Bates, N. R., Bell, S., et al. (1997). *BATS Methods Manual*. Woods Hole, MA: JGOFS Planning Office.

Kobari, T., Honma, T., Hasegawa, D., Yoshie, N., Tsutsumi, E., Matsuno, T., et al. (2020). Phytoplankton growth and consumption by microzooplankton stimulated by turbulent nitrate flux suggest rapid trophic transfer in the oligotrophic Kuroshio. *Biogeosciences* 17, 2441–2452. doi: 10.5194/bg-17-2441-2020

Lee, Z., Weidemann, A., Kindle, J., Arnone, R., Carder, K. L., and Davis, C. (2007). Euphotic zone depth: Its derivation and implication to ocean-color remote sensing. *J. Geophys. Res.* 112:2006jc003802. doi: 10.1029/2006jc003802

Liang, W.-D., Yang, Y. J., Tang, T. Y., and Chuang, W.-S. (2008). Kuroshio in the Luzon Strait. *J. Geophys. Res.* 113:2007jc004609. doi: 10.1029/2007jc004609

Mendonca, A., Aristegui, J., Vilas, J. C., Montero, M. F., Ojeda, A., Espino, M., et al. (2012). Is there a seamount effect on microbial community structure and biomass? The case study of Seine and Sedlo seamounts (northeast Atlantic). *PLoS One* 7:0029526. doi: 10.1371/journal.pone.0029526

Miles, J. W. (1961). On the stability of heterogeneous shear flows. *J. Fluid Mech.* 10, 496–508. doi: 10.1017/S0022112061000305

Mohn, C., and Beckmann, A. (2002). The upper ocean circulation at Great Meteor Seamount. *Ocean Dynam.* 52, 179–193. doi: 10.1007/s10236-002-0017-4

Morato, T., Varkey, D. A., Damaso, C., Machete, M., Santos, M., Prieto, R., et al. (2008). Evidence of a seamount effect on aggregating visitors. *Mar. Ecol. Prog. Ser.* 357, 23–32. doi: 10.3354/meps07269

Moum, J. N., Farmer, D. M., Smyth, W. D., Armi, L., and Vagle, S. (2003). Structure and generation of turbulence at interfaces strained by internal solitary waves propagating shoreward over the continental shelf. *Am. Meteorol. Soc.* 33, 2093–2112.

Nagai, T., Durán, G. S., Otero, D. A., Mori, Y., Yoshie, N., Ohgi, K., et al. (2019b). How the Kuroshio Current delivers nutrients to sunlit layers on the continental shelves with aid of near-inertial waves and turbulence. *Geophys. Res. Lett.* 46, 6726–6735.

Nagai, T., Clayton, S., and Uchiyama, Y. (2019a). "Multiscale routes to supply nutrients through the Kuroshio nutrient stream," in *Kuroshio Current: Physical, Biogeochemical, and Ecosystem Dynamics*, eds T. Nagai, H. Saito, K. Suzuki, and M. Takahashi (Hoboken, NJ: Wiley), doi: 10.1002/9781119428428.ch6

Nagai, T., Rosales Quintana, G. M., Durán Gómez, G. S., Hashihama, F., and Komatsu, K. (2021). Elevated turbulent and double-diffusive nutrient flux in the Kuroshio over the Izu Ridge and in the Kuroshio Extension. *J. Oceanogr.* 77, 55–74. doi: 10.1007/s10872-020-00582-2

Osborn, T. R. (1980). Estimates of the local rate of vertical diffusion from dissipation measurements. *Am. Meteorol. Soc.* 10, 83–89.

Patterson, M. D., Caulfield, C. P., McElwaine, J. N., and Dalziel, S. B. (2006). Time-dependent mixing in stratified Kelvin-Helmholtz billows: Experimental observations. *Geophys. Res. Lett.* 33:2006gl026949. doi: 10.1029/2006gl026949

Saito, H. (2019). "The Kuroshio: its recognition, scientific activities and emerging issues," in *Kuroshio Current, Physical, Biogeochemical and Ecosystem Dynamics*, Vol. 1-11, eds T. Nagai, H. Saito, K. Suzuki, and M. Takahashi (Hoboken, NJ: John Wiley & Sons).

Sckopke, N., Paschmann, G., Haerendel, G., Sonnerup, B. U. Ö, Bame, S. J., Forbes, T. G., et al. (1981). Structure of the low-latitude boundary layer. *J. Geophys. Res.* 86, 2099–2110. doi: 10.1029/JA086iA04p02099

Shroyer, E. L. (2012). Turbulent kinetic energy dissipation in Barrow Canyon. *J. Phys. Oceanogr.* 42, 1012–1021. doi: 10.1175/jpo-d-11-0184.1

Sibert, J., Holland, K., and Itano, D. (2000). Exchange rates of yellowfin and bigeye tunas and fishery interaction between Cross seamount and near-shore FADs in Hawaii. *Aquat. Living Resour.* 13, 225–232. doi: 10.1016/S0990-7440(00)01057-3

Smyth, W. D., and Moum, J. N. (2000). Length scales of turbulence in stably stratified mixing layers. *Physics Fluids* 12, 1327–1342. doi: 10.1063/1.870385

Smyth, W. D., Moum, J. N., and Caldwell, D. R. (2001). The efficiency of mixing in turbulent patches: inferences from direct simulations and microstructure observations. *J. Phys. Oceanogr.* 31, 1969–1992.

Tanaka, T., Hasegawa, D., Yasuda, I., Tsuji, H., Fujio, S., Goto, Y., et al. (2019). Enhanced vertical turbulent nitrate flux in the Kuroshio across the Izu Ridge. *J. Oceanogr.* 75, 195–203. doi: 10.1007/s10872-018-0500-2

Thorpe, S. A. (1977). Turbulence and mixing in a Scottish Loch. *Philos. Trans. R. Soc. London* 286, 125–181.

Tsai, C. J., Andres, M., Jan, S., Mensah, V., Sanford, T. B., Lien, R. C., et al. (2015). Eddy-Kuroshio interaction processes revealed by mooring observations off Taiwan and Luzon. *Geophys. Res. Lett.* 42, 8098–8105. doi: 10.1002/2015gl065814

Tsutsumi, E., Matsuno, T., Itoh, S., Zhang, J., Senjyu, T., Sakai, A., et al. (2020). Vertical fluxes of nutrients enhanced by strong turbulence and phytoplankton bloom around the ocean ridge in the Luzon Strait. *Sci. Rep.* 10:17879. doi: 10.1038/s41598-020-74938-5

Tsutsumi, E., Matsuno, T., Lien, R. C., Nakamura, H., Senjyu, T., and Guo, X. (2017). Turbulent mixing within the Kuroshio in the Tokara Strait. *J. Geophys. Res. Oceans* 122, 7082–7094. doi: 10.1002/2017jc013049

Uchida, R. N., Hayasi, S., and Boehlert, G. W. (1986). *Environment and Resources of Seamounts in the North Pacific: Proceedings of a Workshop, March 21-23, 1984, Shimizu, Japan*. Washington, D.C: NOAA.

White, M., Bashmachnikov, I., Arístegui, J., and Martins, A. (2007). "Physical processes and seamount productivity," in *Seamounts: Ecology, Fisheries and Conservation*, eds T. J. Pitcher, T. Morato, P. J. B. Hart, M. R. Clark, N. Haggan, and R. S. Santos (Hoboken, NJ: Willey), 65–84.

Woods, J., and Wiley, R. (1972). Billow turbulence and ocean microstructure. *Deep Sea Res. Oceanogr. Abstracts* 19, 87–121. doi: 10.1016/0011-7471(72)90043-5

Zhang, W.-Z., Wang, H., Chai, F., and Qiu, G. (2016). Physical drivers of chlorophyll variability in the open South China Sea. *J. Geophys. Res.* 121, 7123–7140.

Conflict of Interest: The authors declare that the research was conducted in the absence of any commercial or financial relationships that could be construed as a potential conflict of interest.

Publisher's Note: All claims expressed in this article are solely those of the authors and do not necessarily represent those of their affiliated organizations, or those of the publisher, the editors and the reviewers. Any product that may be evaluated in this article, or claim that may be made by its manufacturer, is not guaranteed or endorsed by the publisher.